

I. CALORIMETRY

A. Introduction

The present calorimeter system of LHCb is composed of a Scintillating Pad Detector (SPD), a Preshower (PS), an Electromagnetic Calorimeter (ECAL) and a Hadronic Calorimeter (HCAL). The HCAL is based on the Tilecal technology and contains 1488 cells. It is preceded by the ECAL based on the Shaslik technology and containing 6016 cells. In front of the ECAL, the PS is composed of 6016 tiles matching the geometry of the ECAL. The PS is placed after a lead sheet of 2.5 radiation length and is preceded by another layer of 6016 scintillator tiles, the SPD. The detailed description of the calorimeter system can be found in [2].

The calorimeter system plays a role in photon reconstruction (ECAL), in photon and electron identification (ECAL, PS, SPD), and in the trigger system (HCAL, ECAL, PS, SPD).

For the LOI we have concentrated the studies on the upgrade of the ECAL and HCAL readout at 40 MHz, since we do not exclude removing the SPD and PRS for the upgrade.

- The low level trigger foreseen to replace our present L0 trigger does not require a very strict selection and therefore it can be operated without the PS and SPD.
- It remains to be studied whether the necessary electron and photon identification needed for parts of our upgrade physics program can be achieved without the SPD and PS.

If an upgrade of the SPD and PRS is needed, the modifications to the front-end cards would be very similar to the modifications of the ECAL/HCAL front-end cards described below.

To minimize the required modifications, it is planned, for the upgrade, to keep the present ECAL and HCAL calorimeter modules, their photo-multipliers (PMT), Cockroft Walton bases (CW) and coaxial cables. However, to keep the same average anode current of the phototubes at the higher luminosity, their high voltage (HV) is reduced and therefore the gain of the amplifier integrator in the Front End card will be increased. This is described in section IB.

The racks and crates situated at the top of the calorimeter can be kept as they are, however of course the Front end cards have to be modified to allow a read out at 40MHz. To minimize the number of fibers necessary to read the calorimeters the ADC information is packed using an algorithm similar to the one presently used in the TELL1 calorimeter cards. The new Front End cards are described in section IC.

The decision to keep the calorimeter modules, their PMTs and CW bases assumes that they can operate with the radiation damage corresponding to the foreseen integrated luminosity. This is discussed in section ID.

Because of the higher luminosity, there will be a higher occupancy in the calorimeter cells. This will cause an increase in calorimeter noise due to statistical fluctuation in these underlying events. While the effect is small for the measurement of high E_t photons it is important in the case of low E_t photons. In section IE an estimate of this equivalent noise is given.

B. ECAL/HCAL electronics upgrade: analogue front-end

The analogue signal processing in the present ECAL Front End (FE) board ([1], [2], [3]) is mostly performed by a shaper ASIC that integrates the PMT pulse, which has been clipped at the PMT base. The PMT is located at the detector; the signal is transmitted through a 12m 50 Ω coaxial cable to the FE board located in the crates at the calorimeter platform.

Requirements	
Energy range	$0 \leq E_t \leq 10\text{GeV}$ (ECAL)
Calibration/Resolution	4fC/2.5MeV per ADC count
Dynamic range	4096-256 = 3840 cnts: 12 bits
Noise	$\lesssim 1$ ADC cnt (ENC < 5 – 6 fC)
Termination	$50 \pm 5\Omega$
Baseline shift prevention	Dynamic pedestal subtraction
Max. peak current	4-5 mA over 50 Ω
Spill-over correction	Clipping
Linearity	< 1%
Cross-talk	< 0.5%
Timing	Individual (per channel)

TABLE I. Summary of the requirements for the calorimeter analogue FE.

The PMT gain has to be decreased by a factor 5 with respect to the present operation HV in order to keep the same average current after the increase in luminosity¹. Therefore, this has to be compensated in the electronics and the preamplifier input equivalent noise must be decreased accordingly.

Noise after integration and pedestal subtraction should be at the level of 1 ADC count approximately, corresponding to an input charge of 4fC RMS (compared to 20fC in the present system). Detailed noise analysis shows that total input referred noise voltage of the front-end should be smaller than $1\text{nV}/\sqrt{\text{Hz}}$. This requirement includes not only the input referred noise of the amplifier but any other noise source, i.e. the 50 Ω termination resistor; therefore, a passive termination is not acceptable. Active termination schemes are under study. Because the implementation of an active termination requires a transistor level approach and because the FE board has 32 channels; an ASIC development is under study. It will be described below.

However, it is important to take into account that currently the PMT signal is clipped in the base, i.e. at the detector, and about 2/3 of the signal charge are lost. An alternative solution could consist of removing the clipping of the PM base and perform it after amplifying the signal in the FE card. This would relax by a factor 3 the noise requirement of the front end amplifier, thus allowing a passive termination. Although this solution requires intervention in the detector, the operation is feasible. Such a solution, based on Commercial Off-The-Shelf (COTS) Op Amps and analogue delay lines is also described.

¹ According to Hamamatsu PMT specifications, a 20% gain reduction may be expected per integrated charge of 100C (the expected charge per year in present conditions and worst PMT position).

After analogue signal processing, either with an ASIC or using COTS, the signal must be digitized through a 12 bit ADC at 40 MHz. Baseline candidate is the AD9238 ADC, which is a dual pipeline ADC. Its sampling frequency ranges from 20 to 65 MHz.

Table I summarizes main requirements for the analogue FE of the calorimeter system. Except for PMT current and noise, the other requirements are similar to the ones for the current ECAL front end ([1], [2], [3]).

1. *Integrated implementation*

Active termination avoiding resistor termination and its thermal noise is usually referred as “electronically cooled termination“. Conventionally it is created by an operational amplifier with capacitive feedback. This solution works well, provided that the input signal amplitude is not so large as to produce significant changes in the input amplifier transconductance. In the case of calorimeters for high energy experiments, this may not be the case as large dynamic range is usually required. The ATLAS LAr calorimeter preamplifier creates the electronically cooled termination through a “super common base” input stage with an additional feedback loop [5]. An ASIC in IBM’s 8WL 130nm SiGe process is being designed for the LHC upgrade [6].

The LHCb Preshower chip relies also on a super common base stage [2], however no cooled termination is used in this case because the chip is located in the PM base. The input current is amplified and converted to differential signalling in order to be integrated through a fully differential amplifier with capacitive feedback. Since no dead time is allowed and high quality delay lines can not be easily integrated, the solution adopted for the PS is to alternate every 25 ns between two integrators and to reset one integrator when the other one is active.

The proposed implementation of the ASIC for the calorimeter electronics upgrade is based on a combination of the two previous solutions. In the first place a “super common base” input stage with additional current feedback creates the electronically cooled termination as shown in Fig. 1. Then two alternated switched signal paths are used to integrate and sample the input current with no dead time, as in the Preshower sub-detector.

A first prototype of input stage of the chip including preamplifier and switched integrators has been designed in Austriamicrosystems 0.35 um SiGe BiCMOS technology and submitted to the foundry in June 2010 (Fig. 2). There are a number of key issues to be tested, corresponding to some innovations with respect to the ASICs referred above. On the one hand the amplifier uses current feedback (Fig. 1, left) for several reasons:

- The output is a mirrored current.
- Additional I/O pads are needed for standard voltage feedback [7], but not for current feedback. This makes easier the implementation of a fully differential channel (with pseudo differential input), which may be critical in a FE board with large amount of digital circuitry.
- All nodes have low impedance, and hence less prone to pick up noise.
- ESD robustness is improved since no MOS transistor gate or bipolar base is connected to the input pad (series resistors are not allowed for noise reasons).

Current mirrors are based on active cascode circuits in order to be able to achieve the required linearity, noise and bandwidth.

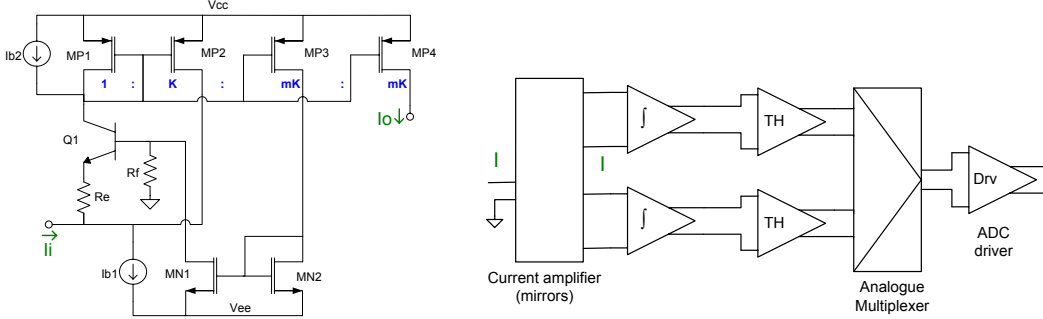


FIG. 1. Super common base amplifier with current feedback (left) and interleaved switched paths (right).

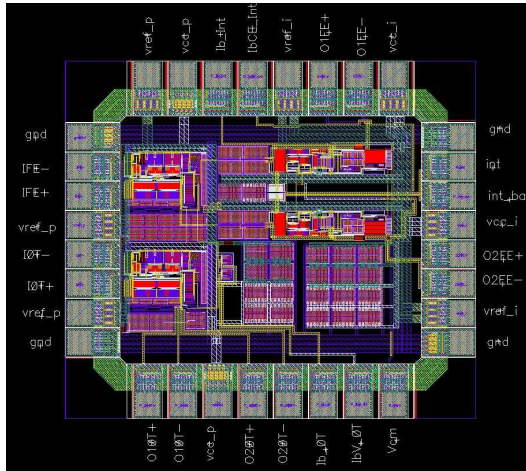


FIG. 2. First ASIC prototype of the input part of the channel.

2. Discrete component implementation

Provided that the clipping line in the base of the PMTs (Fig. 3, left) is removed, noise requirements can be relaxed and line termination can be performed with a resistor. With COTS it is possible to implement a similar scheme as the one already working in the current ECAL. However, there are two modifications compared to the present design: an input low noise amplifier is used, thus reducing the total noise, and the clipping is performed on the electronic card after the input amplifier rather than in the PMT's base. The clipping principle is preserved but the scheme must be adapted because the operational amplifier has a much lower output impedance than the PMT tube.

This option implies an intervention on the PMT's base, but it is reasonably easy to cut a track of the PCB (Fig. 3, bottom left). This reduces the contribution of the Cockcroft-

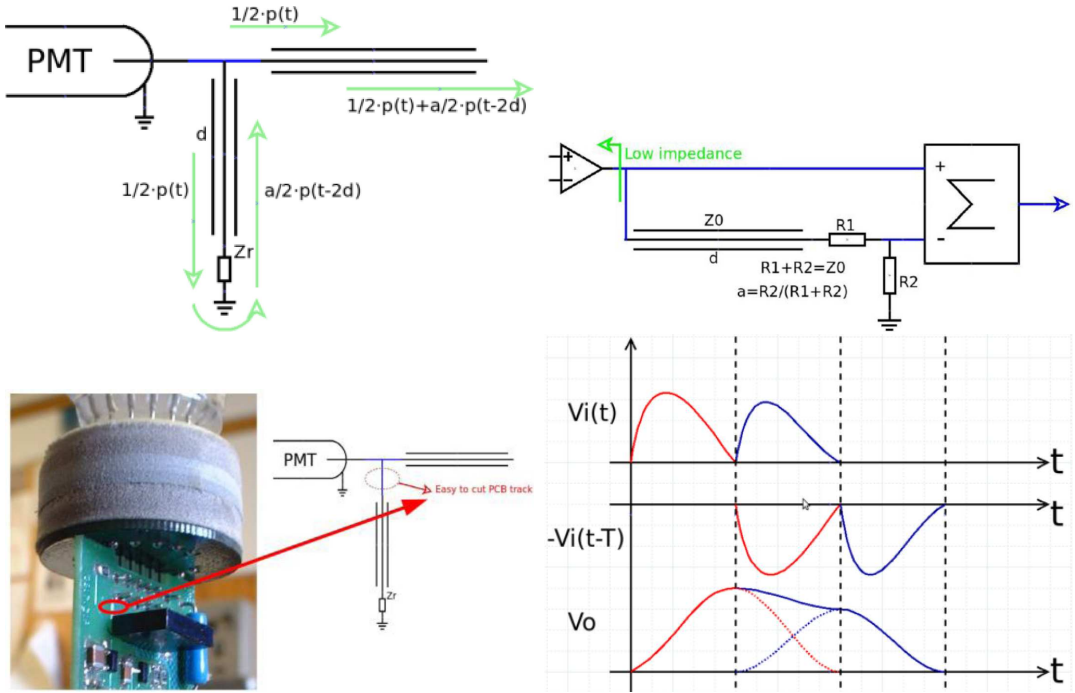


FIG. 3. Principles of Operation for COTS solution. The left drawing and picture show the clipping system (top) and the track on the PMT base that has to be cut to remove the clipping (bottom). The schematics and curves on the right show the system that is used in the COTS implementation to reset the integrator (top) and the resulting integrator output signal (bottom).

Walton induced noise, in case it was coupled after the clipping, since the outgoing signal is larger.

The integration of the signal is done in an operational amplifier and 25ns later a “disintegration” is performed in such a way that at the sampling instant the result of the previous integration is cancelled (Fig. 3, right).

The circuit is made with differential operational amplifiers. This gives two polarities of the signal easing the implementation of the circuit described in Fig. 3.

This scheme helps reducing the pedestal and helps the subtraction algorithm. It also avoids switching currents in the analog power supplies.

A first prototype of the board is already built and the first measurements are being performed.

C. ECAL/HCAL electronics upgrade: the new front-end board

The present front end cards are each connected to 32 PMT signals. They are described in the note [4]. The card main components are

- 8 ASICs each with 4 amplifier integrators.
- 32 Analog devices ADC AD9042.

- 8 FEPGA: FPGA AX250 of ACTEL for signal processing (pedestal subtraction and gain correction in the trigger path). A latency buffer and a derandomiser are used for preparing the data to be read out after reception of a L0 trigger. Injection of test pattern instead of ADC data is foreseen. Each FPGA processes 4 channels.
- 1 TRIGPGA: FPGA AX500 of ACTEL which collects at 40 MHz data, processed in the FEFGAs, from the 32 cells of the card and from $8 + 4 + 1$ cells from neighbouring cards. It selects the highest transverse energy in a cluster of 2×2 cells and sends this information in the trigger path, through the crate backplane and through two trigger validation cards per crate.
- 1 SEQPGA: FPGA APA300 of ACTEL gathers the data readout from the 8 FEPGA serialises them and send them through the backplane to a controller board and then through a fibre to the TELL1 cards.
- 1 FPGA APA150 of ACTEL is used as an interface for ECS (Glue PGA) between the control board of the crate and the front end card to load constants in FPGA, load test patterns, perform spying of data and other functions.

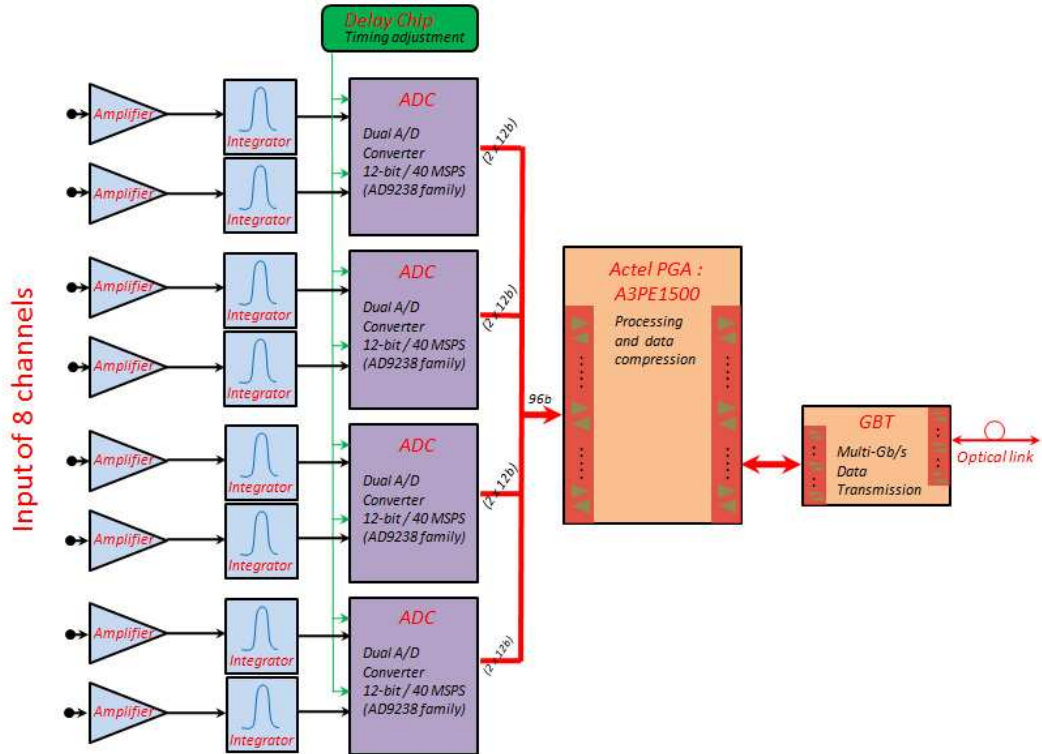


FIG. 4. One front-end block of 8 channels.

In the cards foreseen for the upgrade, the TRIGPGA functionality and therefore probably the FPGA and its firmware will be kept unchanged. This will allow to transmit the high E_t clusters which be used in the low level trigger (see Section ??).

The Glue PGA and its functionality for ECS will probably be kept, while the SEQPGA has no role in a 40MHz readout system.

In the new cards the 32 channels will be grouped in 4 groups of 8 channels (see Fig. 4). In each of the four groups the PMT pulses are amplified and integrated as explained in section IB. They are then converted with 12bit 40MS/s ADC. The ADCs' data will be processed by a single reprogrammable Flash based FPGA of ACTEL. Preliminary studies show that the A3PE1500 has the necessary resources for an 8 channel group. The data will then be sent to the TELL40 boards (see Section ??) by one GBT Fibre system per 8 channel group with a useful bandwidth of 3.2 Gbit/s or 80 bits every 25ns . A schematic diagram of one such group is shown in Fig. 4.

If one would send the 12 bits for each channel, 96 bits/25ns would be needed together with extra information such as the BXID and link identifier. One GBT would then not be enough. However in most cases the ADC data corresponds only to small pulses due to pedestal fluctuation (noise or pile-up). One possibility would be to send only data above a certain Zero-Suppress threshold; however this Zero-Suppression can cause non linearity when measuring calorimeter energy in a 3x3 cluster.

In the upgraded cards we propose to compress the ADC information of 8 channels, in the A3PE1500 FPGA. For each event an 8bit pattern word describe if each ADC is of short data (5 bits transmitted) or long data (the full 12 bits are transmitted). Simulations have shown that using this scheme one GBT per 8 channels is sufficient to transmit the information even in the highest occupancy region of the calorimeter and at the highest luminosity, if the event to event fluctuations are averaged over a large number of events, including events with empty proton bunches in the LHC. It has been verified that the multiplexer cells and memory blocks of the A3PE1500 are sufficient to implement such a scheme.

A prototype of an 8 channel slice of the front end card has been built for tests of the analog and digital part in 2010 and 2011. It is shown in Fig. 5.

D. Radiation issues

At high luminosity operation, the central cells of both ECAL and HCAL will receive significant radiation doses, and their performance will be deteriorated. As the resolution of HCAL central cells is not of critical importance for the detector operation, we consider hereafter only the ECAL performance degradation. The ECAL and HCAL front-end electronics is located above the detector. The dose expected after an integrated luminosity of 5fb^{-1} is of 1krad in the crate vicinity. The components will be radiation tested and chosen to cope with this level[2].

The predictions for the doses received by ECAL can be found in [2], [8]. After 10fb^{-1} , at the innermost cells it reaches $\sim 1.2\text{Mrad}$ at the depth of 6 – 10cm from the front face of the detector (electromagnetic shower maximum), and is $\sim 0.6\text{Mrad}$ at its rear surface, where photomultipliers are installed (see Fig. 3.10 of [2]). Most of the dose ($\sim 75\%$) comes from hadrons.

From the point of view of radiation tolerance, the following parts of ECAL should be considered:

- Optical elements of the calorimeter modules: loss of transparency and light yield of the scintillator tiles and wavelength shifting fibres (WLS);
- Photomultipliers: degradation of entrance window transparency;

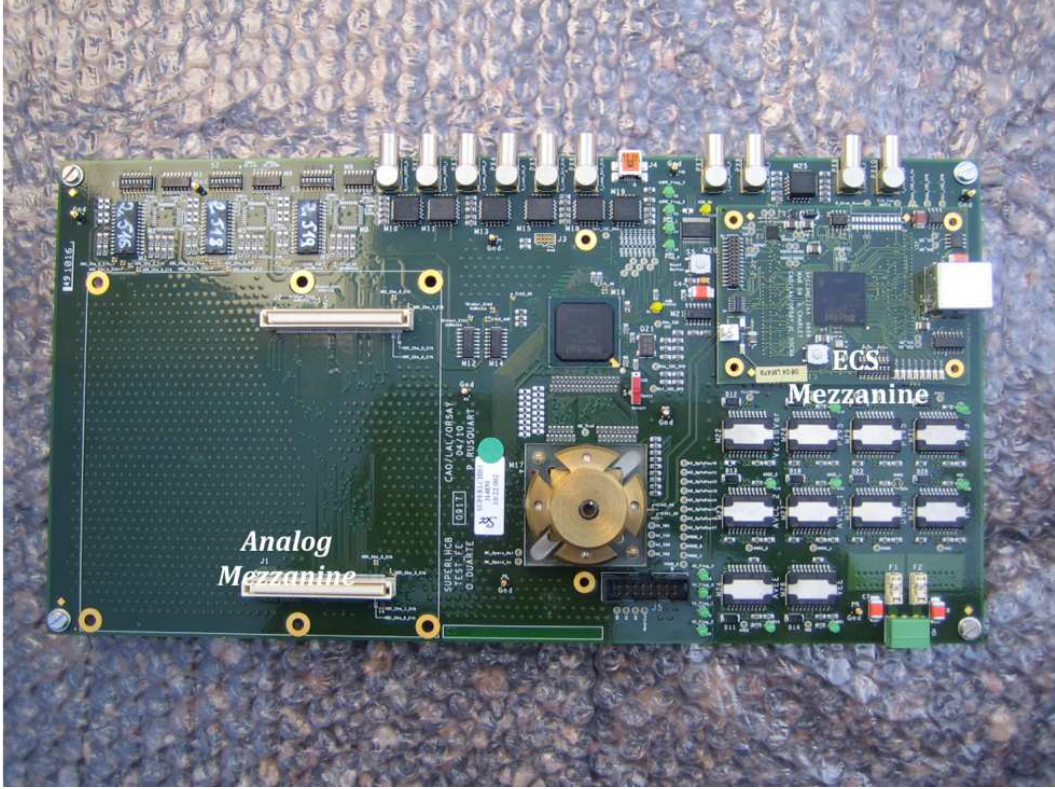


FIG. 5. Picture of the digital electronics first prototype.

- CW bases of photomultipliers: radiation damage of electronic parts.

The radiation damage of the optical elements of the modules, as well as that of the PMT entrance window, will lead to the degradation of the detector sensitivity and energy resolution (now $N_{PHE} \sim 3000 \text{ph.e.}/\text{GeV}$ and according to test beam measurements on a single module, $\sigma(E)/E = 10\%/\sqrt{E(\text{GeV})} \oplus 0.8$ [10]).

In case of degradation above a certain limit, the innermost modules can be replaced: such a possibility is implemented in the mechanical design of ECAL [2].

The radiation damage of the CW bases leads to incorrect (and, in general, unstable) HV values at PMTs.

1. Outcome of the previous tests

Module optics

The radiation resistance of the LHCb ECAL modules was studied during the R&D phase of the project[9]. The most important test was carried out at LIL (LEP Injector Linac) in 2002.

Two modules were irradiated with a 500 MeV electron beam up to a dose of $\sim 5 \text{Mrad}$ at the shower maximum, which, according to the simulation, corresponds to an integrated luminosity of 40fb^{-1} . Then the light yield and transparency of scintillator tiles and WLS

fibres were determined by means of a radioactive source scan. The measurements were performed several times from 7 to 2000 hours after the irradiation; a significant annealing effect was observed.

The values taken after 2000 h annealing were used as an input to the simulation of response to electromagnetic showers obtained with GEANT4. For the calculation of the light yield at intermediate doses, the exponential interpolation was used. The results are shown in Fig. 3.12 of [2]. One can see that at 5Mrad the predicted degradation is such that the light yield becomes 40% of that before irradiation. The degradation of the resolution consists mainly in an increase of the constant term, showing approximately a linear dependence on the dose. At 5 Mrad the constant term becomes $\sim 3\%$ (0.8% before irradiation).

There are 32 spare modules of the inner type, which is, according to these results, enough for the replacement of the most irradiated modules, if it will be found necessary.

PMT entrance window and CW bases

The HAMAMATSU R7899-20 PMTs used in the LHCb ECAL are specially designed to work in high radiation background and their entrance window is made of special material. The CW generator circuit is also radiation tolerant: it is designed such that it is not sensitive to the characteristics of its active elements, and remains operational even with significantly damaged components. In addition, the components with lower degradation rate were specially selected[11].

In order to measure the radiation tolerance of photomultipliers and CW bases, the irradiation tests were conducted at IHEP (Protvino) in 2010. The samples were installed behind a 22cm thick steel converter and irradiated by the 50GeV proton beam of the IHEP U-70 accelerator up to the doses of 1-2Mrad, depending on the sample position. The duration of the test was 3 days; the parameters of the samples were then measured in several days after the end of the irradiation, without a long annealing period. These results can be considered only as a lower limit for the radiation tolerance.

During the test, the HAMAMATSU PMT sample received ~ 1.9 Mrad, equivalent to 6 years of operation at 5fb^{-1} per year; then, after 11 days, its window transmittance was measured with a spectrophotometer, and compared to the window of a non-irradiated sample. In the wavelength range from 500 to 550nm the loss of transmittance did not exceed 5%. The conclusion is therefore that the radiation tolerance of the PMT entrance window is sufficient to work during the full upgrade program period.

To study the radiation hardness of CW bases, three samples were installed at the beam and powered up. The output voltage (initially $\sim 950\text{V}$) was monitored during the tests and stable until failure. The failure occurred at doses between 1.4 and 1.7 Mrad. Our conclusion is that the CW bases of photomultipliers are radiation tolerant at least till the dose of 1 Mrad, which is sufficient even for the innermost cells to survive during 2 year at 5fb^{-1} . The replacement of CW bases can be performed during annual shutdown periods and 500 spare CW bases are enough for the full upgrade program.

2. Future tests

Following these initial tests, there remained some uncertainty on the radiation tolerance of the ECAL modules for the following reasons. First, the tested optical components are not of exactly the same type as the ones finally used in the ECAL construction. Second, the irradiation was performed in the electron beam, while in real conditions it will be mostly hadronic; this may imply different degree of damage and different depth of annealing. The light yield and transmission of the optical components is affected as function of the z coordinate along the module. Simulations are used to combine these effects with fluctuations in shower depth, thus calculating the degradation in resolution. This simulation is a third cause of inaccuracy.

Practically, it translates into the uncertainty in module replacement frequency and total number of spares needed.

Taking into account all the facts mentioned above, it was decided to perform a new series of tests, irradiating spare ECAL modules in the hadron beam. Two ECAL modules of inner type were placed for irradiation into the LHC tunnel. The position (near the LHCb interaction point, at a distance of $\sim 4\text{m}$ along the Beam 2 direction, and at 15cm from the beam line) is chosen such that the dose received by the test modules during the LHC operation will be ~ 10 times more than that for the innermost modules of ECAL. It is therefore expected that by the end of 2011 the test modules will get a dose corresponding to approximately 1 or 2 years of 5fb^{-1} . The decision will be taken after measurement of characteristics of the test modules, which could take place in 2012-2013 at a SPS electron beam. At this point, there is still enough time to produce extra spare modules if it is found necessary.

E. Pile-Up effect

The luminosity increase foreseen for the LHCb upgrade will lead to a large average number of interactions per crossing and therefore to an increase of the event multiplicity. This may affect the electromagnetic calorimeter (ECAL) energy and position resolutions by shifting on average the energy measurements and smearing the reconstructed energy and position of the clusters.

Several methods have been used to estimate the effect and the one presented here relies on real data recorded with the calorimeter system at 3.5TeV. The energy is lower than what is expected for the upgrade but the estimation is based on real data and on that aspect it is more realistic than estimations from simulations².

1. Noise estimation method:

The method consists in storing the signal seen by the 6010 cells of the ECAL for a large minimum-bias data sample and before zero-suppression. This is possible as the LHCb

² The event P_t spectrum should not change with the energy, but we expect an increase of the multiplicity of $\approx 20\%$, according to the Pythia simulations, between 3.5TeV and 7.0TeV in beam energy.

electronics and acquisition only perform a compression of the data without loss of information, the zero-suppression being done at the reconstruction level. Using the raw data that are presently available, the reconstruction is run again after relaxing the zero-suppression threshold. To generate a high luminosity event, several minimum-bias events are piled-up by adding the ADC counts measured for each cell of the calorimeter.

The number of minimum bias events added depends on a random number of interactions per beam crossing given by a Poisson law as function of the luminosity. Two quantities are finally extracted per cell: the average number of ADC counts seen that is a measurement of the transverse energy (the photo-multipliers gains are adjusted with a $\sin(\theta)$ law in order to provide at the trigger level an E_t measurement) and the RMS of the fluctuations of this signal. The ECAL cells are such that a typical electromagnetic shower is contained in a cluster made of 3x3 cells. The same quantities as previously mentioned are also extracted for such clusters.

2. Results

Figure 6 shows the results at the maximum luminosity expected for the first phase of the upgrade, $10^{33}\text{cm}^{-2}\text{s}^{-1}$. The electromagnetic calorimeter energy resolution may be expressed by

$$\frac{\sigma(E)}{E} = \frac{10\%}{\sqrt{E(\text{GeV})}} \oplus 1.5\% \oplus \frac{0.0025 \times \text{RMS}}{E \sin(\theta)} (\text{Pile-up}) \oplus \frac{0.01}{E \sin(\theta)} (\text{Noise}) \quad (1)$$

$\mathcal{L}(\text{cm}^{-2}\text{s}^{-1})$	2×10^{32}	5×10^{32}	10^{33}	2×10^{33}
<i>RMS</i>	12	15	18	22
$0.0025 \times \text{RMS}$	0.030	0.038	0.045	0.055

TABLE II. Average RMS of the pile-up contribution to the signal of the ECAL cell signal at different luminosities. The numerator of the contribution to the resolution is also given.

$\mathcal{L}(\text{cm}^{-2}\text{s}^{-1})$	2×10^{32}		10^{33}	
	Total	Pile-up	Total	Pile-up
$B \rightarrow D^*(D\gamma)K$	7.4%	4.7%	14.3%	13.1%
$B \rightarrow \phi\gamma$	2.3%	0.5%	2.7%	1.5%

TABLE III. Energy resolution for two types of photon reconstructions at low (400MeV, $B \rightarrow D^*K$) and high (3.5GeV, $B \rightarrow \phi\gamma$) E_t at an angle of 100mrad. The overall resolution and the pile-up contribution are given at the present nominal luminosity and at the expected one for the first phase of the upgrade.

where the pile-up contribution is extracted from the present analysis and the noise contribution is the one measured at the pit with the present system. Notice that the ADC count being in E_t those contributions depend on the angle of the cell with respect to the

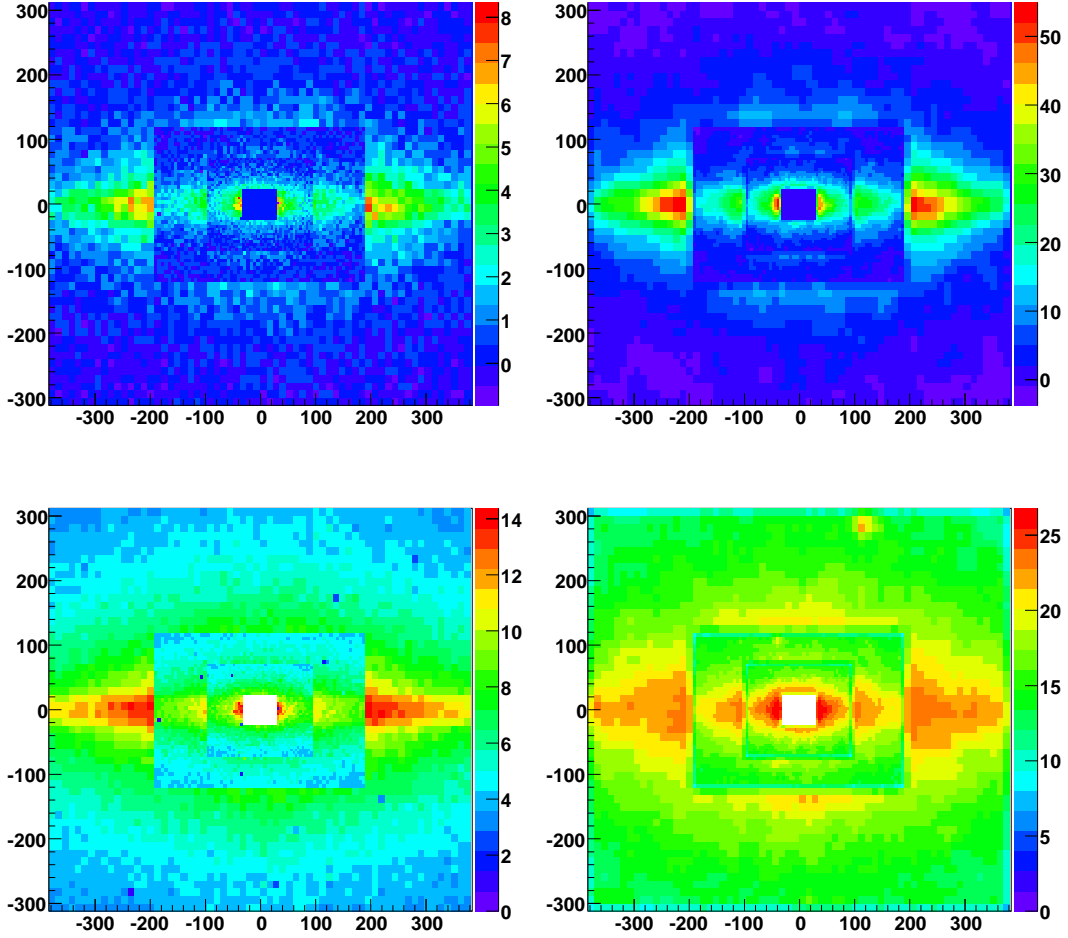


FIG. 6. 2D maps (x and y axis are in cm) of the average signal in ADC counts (top) and of its distribution RMS (bottom) for the 6016 cells of the ECAL. The maps are produced from a sample of 100000 generated events faking a luminosity of $10^{33}\text{cm}^{-2}\text{s}^{-1}$. The left maps show the average signal and RMS per cell, the right ones represent the same quantities for 3×3 clusters, the position of the cluster on the map being the one of the central cell of the cluster. The bottom right plot gives the P_t fluctuations (in ADC counts) that we can expect on the calorimeter surface. Multiplying by 2.5MeV gives the corresponding information in MeV.

beam axis. The extra energy measured can on average be removed, but the resolution is degraded according to the RMS of the pile-up contribution. Table II lists the numerators to the pile-up contribution to the ECAL resolution for luminosities ranging from 2×10^{32} up to $2 \times 10^{33}\text{cm}^{-2}\text{s}^{-1}$ and averaged over the calorimeter cells.

The degradation on the resolution could also be viewed for two different photon reconstructions, at low and high E_t and depends on the photon angle (according to formula 1) and table II (for the pile-up contribution RMS). The typical E_t for the channel $B \rightarrow D^*K$ is 400MeV and it is around 3.5GeV in the $B \rightarrow \phi\gamma$ decay. Table III shows the degradation of the energy resolution at an angle of 100mrad (the total angular acceptance covering the

region $[30, 250]\text{mrad}$) and for luminosities of 2×10^{32} and $10^{33}\text{cm}^{-2}\text{s}^{-1}$. As expected, the high E_t reconstruction does not suffer from the pile-up effect. At low E_t , it becomes the largest contribution to the resolution.

-
- [1] The LHCb Collaboration, The LHCb detector, JINST 3 S08005, 2008
 - [2] S. Amato et al., LHCb calorimeters technical design report, CERN-LHCC-2000-036
 - [3] C. Beigbeder-Beau et al., The front-end electronics for LHCb calorimeters, Note LHCb-2000-028
 - [4] C. Beigbeder-Beau et al., Description of the ECAL/HCAL front-end card, Note LHCb-2003-036 (EDMS 909465)
 - [5] R. L. Chase and S. Rescia, A linear low power remote preamplifier for the ATLAS liquid argon EM calorimeter, IEEE Trans. Nucl. Sci., 44:1028, 1997
 - [6] N. Dressnandt, M. Newcomer, S. Rescia and E. Vernon, LAPAS: A SiGe Front End Prototype for the Upgraded ATLAS LAr Calorimeter, TWEPP-09: Topical Workshop on Electronics for Particle Physics, Paris, France, 21 - 25 Sep 2009
 - [7] F. Yuan, Low-Voltage CMOS Current-Mode Preamplifier: Analysis and Design, IEEE Transactions on Circuits and Systems, Vol. 53, No. 1, 2006
 - [8] G. Corti, L. Shekhtman, Radiation background in the LHCb experiment, LHCb-2003-83, 22 Septembet 2003
 - [9] Arefev et al, Beam Test Results of the LHCb Electromagnetic Calorimeter, LHCb-2007-149
 - [10] Arefev et al, Design, construction, quality control and performance study with cosmic rays of modules for the LHCb electromagnetic calorimeter, LHCb-2007-149
 - [11] Arefev et al, Design of PMT base for the LHCb electromagnetic calorimeter, LHCb-2003-150